COMMUNICATIONS IN SCIENCE AND TECHNOLOGY
Homepage: cst.kipmi.or.id

Synthesis of Si/SiO_2 core/shell fluorescent submicron-spheres for monitoring the accumulation of colloidal silica during the growth of diatom *Chaetoceros sp.*

Luu Manh Quynh[a,*], Hoang Van Huy[a], Nguyen Duy Thien[a], Le Thi Cam Van[b], Le Viet Dung[b]

[a]*Center for Materials Science, Faculty of Physics, VNU – University of Science – 334 Nguyen Trai, Thanh Xuan, Hanoi 100000, Vietnam*

[b]*Faculty of Fisheries, Vietnam National University of Agriculture – Trau Quy, Gia Lam, Hanoi 100000, Vietnam*

Article history:
Received: 21 December 2021 / Received in revised form: 2 March 2022 / Accepted: 3 March 2022

Abstract

Marine diatoms play a very crucial role in carbon export, and current food-web and become an important factor in global silica cycle. This then has made the mechanism of their biosilicification interesting to be a research subject. The classical theory states that the silica metabolism has been originated from the absorption of silicate ions, which might not give a suitable explanation for the solid silica silicification. In this study, mono-disperse Si/SiO_2 fluorescent submicron-spheres were synthesized in aqueous solution, and applied in monitoring the extracellular solid silica accumulation of *Chaetoceros sp.* diatom. The Si/SiO_2 submicron particles emitted light-blue color with the spectrum centered at 440 nm under the excitation of 365 nm UV light, similar to the typical excitation/emission pair of the DAPI fluorophore (excitation/emission: 358 nm/461 nm). The fluorescence-microscopic investigation showed that the Si/SiO_2 particles delocalized on the diatoms' surface and increased a silicic-acid-level surrounding the microalgae. As a consequence, the growth rate of the diatoms increased as the concentration of the SiO_2 particles was at 120 mg/L, and reached 1.5 times higher than the growth rate calculated from the F2 media. The study not only introduces a new aspect to the extracellular metabolism of microalgae biosilicification corresponding to the global silica cycle, but also presents a new-type of culturing media using SiO_2 nanoparticles for diatom cultivation, which increases the growth rate of artificial diatom-culturing for further applications.

Keywords: Si Quantum dots; SiO_2 submicron-spheres; diatom cultivation; extracellular biosilicification; silica cycle

1. Introduction

Being responsible for 40% of the oceanic primary productivities, diatoms are of the most population contributors to global phytoplankton, leading them to play a significant part of a core source of carbon export [1], current marine food-webs [2] and silica cycle [3]. Their abundant fatty acid and protein have expanded their bioactivities aiding in aquaculture feeding system [4,5], human health and cosmetic [6,7]. Besides, their frustule secondary-structural silica cell wall is functioned to create different porous silica-configurations in nanoscale with high surface area, which are promising candidates for any extended applications in modern technologies, such as wastewater treatment [8], drug delivery [9,10], biosensing [11,12] and energy production[13].

In view of the above mentioned magnificent values, diatoms have been isolated and cultivated intensively [14,15]. Based on the culturing mediums as found by Provasoli [16] and Guillard [17], additional nutrients have been added to enrich individual element content [18,19] or to investigate the growth rate [19,20] of diatoms. Silica-containing chemicals, commonly being Na_2SiO_3 in classical culturing media [17-20], would be the indispensable nutrient-feeding components recommended in diatom culturing media. As a consequence, increasing the silica consumption is required for the growth rate during a diatom cultivation process. However, the concentration of silicate ions is generally bounded under 100μM [17-19,21]. At higher concentration, the silicate ions might precipitate with other nutrients, such as Fe^{3+}, Co^{2+} and Cu^{2+}, present in the culturing media, leading to the lack of metal nutrients. Rosaline et al. showed that the elevating concentration of silica in culturing media - up to 2 mM - indicated the low growth rate and smaller size of the diatoms [20]. Hence, further increasing the growth rate of the diatom cultivation has been challenging.

By a symbiosis cultivation process with a coccolothophor, Okcu et al. presented a method to increase the silica consumption in the culturing solution to improve the diatom growth rate [22]. In the article, under rich CO_2 condition, the NO_3^- formed during the coccolothophor development reacted with the $Si(OH)_4$ in solution, created colloidal SiO_2 and indicated the elevating growth of the diatoms [22]. In another study under a scanning microscope, Ikeda found out that the colloidal SiO_2 particles at sub-micron sizes accumulated on the surface of the diatoms [23]. The author suggested that the small size of colloidal SiO_2 could assist the development of the

* Corresponding author. Tel.+84-98-442-4843
Email: luumanhquynh@hus.edu.vn
https://doi.org/10.21924/cst.7.1.2022.661

marine microalgae. Besides, a new insight of biosilicification has also been proposed by Ikeda in two steps: extracellular silica absorption and intracellular silica cell-wall deposition. The intracellular metabolism agrees with the classical theory of diatom silicification in which the absorbed $SiO_2(OH)_2^{2-}$ ions are transported to silica deposition vesicles (SDV) where the silica polymerization process and exocytosis to cell wall occur [24].The classical theory states that the extracellular silicic acids in the form of $SiO_2(OH)_2^{2-}$ ions are absorbed through the cell wall by a silicic-acid receptors (Si-receptors) [24,25]. In contrast to this, Ikeda recommended that the silicic acid in the form of $Si(OH)_4$ formed colloidal SiO_2 particles, immobilized on diatoms' surface before being absorbed into the cell [23]. This suggestion explained the presence of colloidal SiO_2 on the diatom surface, but did not clarify the transportation of colloidal SiO_2 through the cell wall and becoming intracellular $SiO_2(OH)_2^{2-}$ ions.

The localization of SiO_2 nano-particles could be monitored under a fluorescent microscope by implanting organic [26] or inorganic [27] fluorophores into the particles. Of the fluorophores implanted SiO_2 particles, owing to their high quantum luminosity and stability, quantum dots / SiO_2 particles in core/shell structures become the important candidates as potential probes for bioimaging [27]. Belonging to these core/shell systems, biocompatible Si/SiO_2 core/shell nanoparticles were synthesized by a simple hydrothermal process emitting the light-blue color at around 450 nm under 360 nm excitation light-beam [28]. These excitation-emission wavelengths were close to those of the typical dye in biology 4,6-diamidino-2-phenylindone (DAPI – excitation/emission: 358 nm/461 nm). Therefore, they were sufficient for monitoring the solid silica extracellular delocalization on diatom under microscope.

In this work, aiming to study the extracellular metabolism of colloidal SiO_2, luminescent submicron SiO_2 spheres were synthesized and monitored the delocalization of luminescent sub-micron silica particles on the surface of the diatom under a fluorescent microscope during the growing process of *Chaetoceros sp.*. With this, the role of submicron colloidal SiO_2 particles as silica-consumption for diatom growth was investigated as well.

2. Materials and Methods

2.1. Synthesis of Si/SiO₂ submicron-spheres

Si/SiO_2 submicron-spheres were synthesized through two steps: (i) the preparation of Si quantum dots by a hydrothermal process and (ii) coating the quantum dots with a SiO_2 submicron spherical cover. In the first step, the typical hydrothermal process of Si quantum dots synthesis has been described elsewhere by Zhong [29]. In detail, 3 mL of (3-aminopropyl) triethoxysilane (APTES – MERCK CAS 919-30-2) was added into a three-neck beaker that contained 1 g trisodium citrate (TSC – MERCK CAS 6132-04-3) diluted in 30 mL distill water. The solution was stirred for 10 min before being transferred to a Teflon autoclave. It then was sealed in a stainless steel cover for a 12h hydrothermal process at 170°C. After the hydrothermal process, the byproducts from the reaction were filtered by a 3.5 kDa cellulose dialysis tube under vigorous stirring at 4°C in 24 h. The product as-received was labeled as "Si QDs". In the second step, the SiO_2 coating of the Si QDs was carried out following a modified-Stober hydrolysis of tetratethyl orthosilicate (TEOS – MERCK CAS 78-10-4) [30]. Typically, 5 mL homogenous solution containing 7.4 mg TSC, 1 mL ammonium hydroxide solution 25% (Sigma Aldrich CAS 1336-21-6) and 3.75 mL Si QDs solution from 1st step was pipetted into 20 mL mixture of 50/50 methanol/ethanol. After 5 min., 2.5 mL TEOS was added and kept under vigorous stirring for 4 h. The product was washed by centrifugation, collected in aqueous solution and labeled as "Si/SiO_2 spheres" before any investigations.

The second step was applied for the synthesis of SiO_2 submicron spheres without the Si QDs at the core. The SiO_2 particles as-received had the same size and shape with those of the Si/SiO_2 spheres (data not showed); and later were used in diatom growth.

The X-ray diffraction (XRD), Fourier transformed infrared (FTIR) spectra, photoluminescence (PL) and scanning electron micrographs (SEM) of the Si QDs and Si/SiO_2 spheres containing samples were investigated respectively by Bruker D5005 - Siemens, Jasco FT/IR 4700 – Horiba, Prolog 3 – Horiba spectrometers and a Nova nanoSEM 450 – FEI electron-microscope at Center for Materials Science, Faculty of Physics, VNU – Hanoi University of Science. The transmitted electron microscopic (TEM) image of the Si QDs was observed by a FEI Technai transmission electron microscope (TEM) at Institute of Physics, Vietnam Academy of Science and Technology.

2.2. Culturing media preparation for Chaetoceros sp. culturing

Chaetoceros sp. species was purchased from the Aquaculture Research Institute III, Nha Trang and was checked for its size, shape and concentration under a Neubauer counting chamber. All chemicals (shown in Table 1) were purchased from MERCK in analytical grade for synthesis. The Na^+ added compositions $NaNO_3$ (CAS 7631-99-4), NaH_2PO_4 (CAS 10049-21-5) and $Na_2EDTA.2H_2O$ (CAS 6381-92-6); metals containing the compositions of $FeCl_3.6H_2O$ (CAS 10025-77-1), $CuSO_4.5H_2O$ (CAS 7758-99-8), $ZnSO_4.5H_2O$ (CAS 7446-20-0), $CoCl_2.6H_2O$ (CAS 7791-13-1), $MnCl_2.4H_2O$ (CAS 7773-01-5) and $Na_2MoO_4.2H_2O$ (CAS 10102-40-6); the vitamins Thiamin.HCl (CAS 67-03-8), biotin (CAS 58-85-5) and B_{12} (CAS 68-19-9) in reagent grade. The culturing media for the diatom cultivation was prepared following the F2 published by Guillard [17] with the modification on silica source. Four culturing media were applied to investigate the role of solid-silica concentration on the development of the diatoms during cultivation. Conventional F2 was the first culturing media as a control test. In other three media, the silica source Na_2SiO_3 was substituted by different amount of submicron sphere silica with different concentrations labeled as $15SiO_2$, $30SiO_2$ and $120SiO_2$ corresponding to the added 15 mg, 30 mg and 120 mg of solid-silica SiO_2 (Table 1). After vigorous stirring with no aggregation was experienced, 1.2×10^6 cells/mL *Chaetoceros sp.* diatoms were added into the media. The ambient temperature, illumination, air supply conditions were kept the same during the diatom growth. pH value of the diatoms containing growth solution was monitored throughout the

culturing progress and the same indoor-culturing installation was reported elsewhere [31].

Table 1. Composition for 1 L culturing media

Composition	Conventional F2	$15SiO_2$	$30SiO_2$	$120SiO_2$
Silica source				
Na_2SiO_3	30 mg (107 µmol Si)	0	0	0
SiO_2 spheres	0	15 mg (250 µmol Si)	30 mg (500 µmol Si)	120 mg (250 µmol Si)
Na^+ added composition				
$NaNO_3$	150 mg (1.675mmol)			
NaH_2PO_4	10 mg (72.5µmol)			
$Na_2EDTA.2H_2O$	8.7 mg (23.4µmol)			
Metals and trace metals				
$FeCl_3.6H_2O$	6.3 mg (23.3 µmol)			
$CuSO_4.5H_2O$	0.0196 mg (0.079 µmol)			
$ZnSO_4.5H_2O$	0.044 mg (0.153 µmol)			
$CoCl_2.6H_2O$	0.020 mg (0.085 µmol)			
$MnCl_2.4H_2O$	0.360 mg (1.830 µmol)			
$Na_2MoO_4.2H_2O$	0.0126 mg (0.052 µmol)			
Vitamins				
Thiamin. HCl	0.2 mg			
Biotin	1.0 µg			
B_{12}	1.0 µg			

2.3. Monitoring the delocalization of Si/SiO_2 submicron-spheres during the growth of diatom

The silica extracellular absorption of the *Chaetoceros sp.* diatoms during cultivation was obtained under the fluorescent microscope with the excitation/emission filters of DAPI (excitation/emission: 358 nm/461 nm). 30 mg of Si/SiO_2 – about 500 µmol of Si – was added in the F2 culturing media in the substitution of Na_2SiO_3 (same amount with the $30SiO_2$ media). 0.5 mL diatoms containing samples right after the diatoms being added, and after 1 h, 2 h, and 4 h growing they were collected directly from the culturing beaker and had the microscopic images observed under an AXIO SCOPE 3, Carl Zeiss fluorescent microscope.

3. Results and Discussion

Figure 1 presents the XRD patterns and FTIR spectra of the Si QDs and Si/SiO_2 spheres containing powders. The XRD pattern of Si QDs exhibited a broad peak centered at 21.1° corresponding to the amorphous phase of the particles [28,33]. On the FTIR investigation, the characteristic vibrations of APTES attributing to the N-H wagging arose at 758 cm^{-1}, 1484 cm^{-1} and 2881 cm^{-1} in the spectrum of Si QDs and disappeared in the spectrum of Si/SiO_2 spheres corresponding to the coating effect of the SiO_2 cover. Besides, the strong IR absorption at 1064 cm^{-1}, 1024 cm^{-1} related to the Si-O-Si stretching vibration of APTES molecules agreed with earlier published studies [26,32,33].

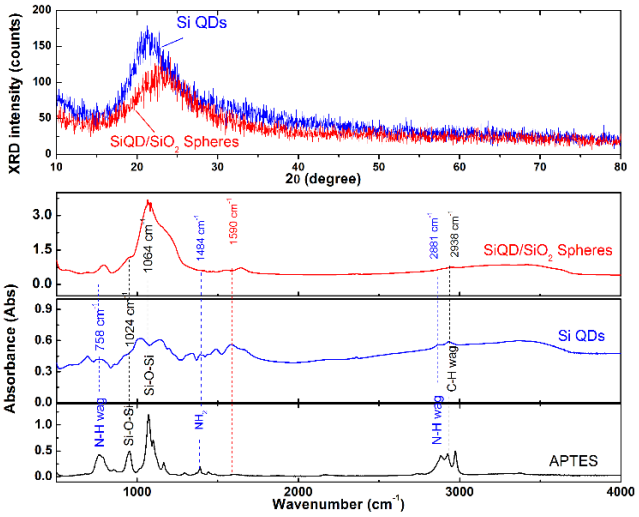

Fig. 1. XRD patterns (upper panel) and FTIR spectra (lower panel) of Si QDs and Si/SiO_2 Spheres containing samples

The Si QDs had the size of 40 nm (Figure 2A), and were mostly in spherical shape in which 4 nm Si nanocrystals were covered by SiO_2 layer (Figure 2B). This structure was representative to the structure of the Si QDs synthesized by hydrothermal method [29,33] where the Si-O linkages from the APTES molecules were reduced to Si seed by TCS under the high pressure of saturated vapor at 170°C in the autoclave. After the formation of the Si seed, silane groups from the APTES were immobilized on the Si surface and formed Si-O stable cover, followed by the bonding of the 3-aminopropyl tails ($-C_3H_6-NH_2$) [26,33]. As a result, the N-H bonds still existed in the Si QDs, as discussed above by the FTIR in figure 1.

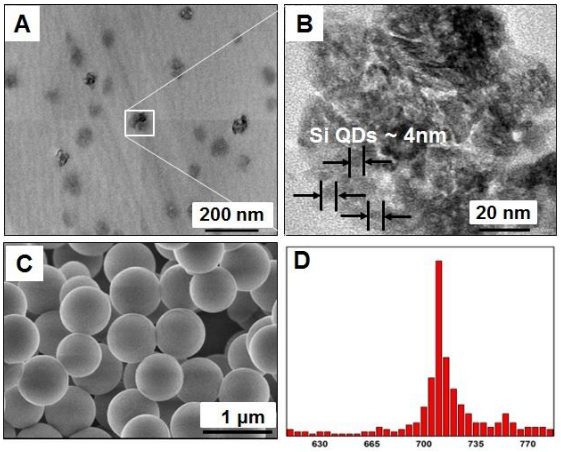

Fig. 2. TEM micrographs of Si QDs at lower magnification (A) and higher magnification (B). SEM image of Si/SiO_2 spheres (C) and their size distribution (D).

The Si-O linkage from the Si QDs particles plays a seed role for the growth of the SiO_2 thicker layer on the surface of the particles in the progress of Si/SiO_2 synthesis [26,33]. Figure 2C shows that the Si/SiO_2 colloids are mono-disperse in a spherical shape with homogenous size. Their size distribution is concentrated at 720 nm with a very narrow deviation (Figure 2D). This submicron size is close to the size of the silica clusters accumulated on the surface of the marine diatom in the

study of Ikeda [23], which would be convenient for an investigation of the solid silica extracellular metabolism of the diatoms

To study the microalgae biosilicification by fluorescent microscope, the photoluminescence of the Si/SiO_2 was investigated. Under the excitation of ultraviolet light, the particles emitted light-blue color with the spectra centered at 440 nm (Figure 3). As the excitation wavelength changed from 250 nm to 400 nm, the fluorescent intensity at 440 nm was measured and the photoluminescence excitation (PL excitation) spectrum was achieved. As shown in figure 3, this spectrum shows the excitation wavelength of 365 nm where the highest luminescent intensity is being observed. The photoluminescence of the Si/SiO_2 is similar to the one in the Si QDs obtained by other authors [27,32] witnessing that the Si QDs are successfully covered into the SiO_2 coat.

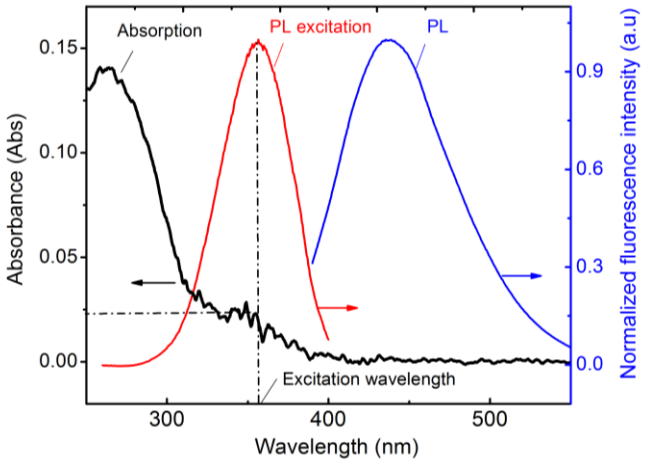

Fig. 3. Absorption, Excitation (PL excitation) and Photoluminescence (PL) spectra of the Si/SiO_2 spheres containing solution.

The quantum yield (QY) of the Si/SiO_2 spheres was estimated indirectly by comparing with the standard fluorophore Rhodamine B by following formula.

$$QY\% = QY\%_s \frac{I^{PL} / 1-10^{Abs}}{I_s^{PL} / 1-10^{Abs_s}} \quad (1)$$

where the I^{PL}, Abs, I_s^{PL}, and Abs_s are the mean photoluminescence intensity and absorbance at the excitation of the Si/SiO_2 containing solution and Rhodamine B. The $QY\%_s$ is the absolute QY of Rhodamine B taken from the reference and being 0.91 [35]. Following to the formula, the QY of the Si/SiO_2 was determined to be 14%. The obtained QY was lower than that of earlier published result by Phan [36], which might correspond to the thick SiO_2 shell that cover the Si QDs surrounding. However, with this QY value, the Si/SiO_2 submicron spheres are still sufficient to be a convenient fluorescent probes to investigate the delocalization of the solid silica on *Chaetoceros sp.* diatoms.

Under a bright-field mode, the positions of the diatoms were visible (Figure $4A_1$-D_1). Their sizes were typically 2-3 µm similarly to other publications [1,2,23]. The same imaging sections were observed under fluorescence mode to achieve the distribution of the blue-light emitting Si/SiO_2 spheres (figure $4A_2$-D_2). It was visualized that, after being added to the culturing solution that contains *Chaetoceros sp.* cells, the Si/SiO_2 submicron spheres were dispensed into the solution followed by the weak luminescence of the samples (figure $4A_2$).

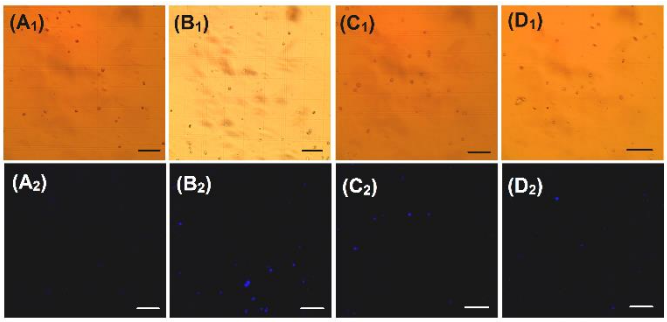

Fig. 4. Bright field – BF (upper panel) and fluorescent – FL (lower panel) microscopic images of the *Chaetoceros sp.* cells containing solution right after the diatoms being added (A), and after 1h (B), 2h (C), 4h (D) cultivation. The scale bars in the image are 5 µm.

The diatom growth is required silica in soluble phase [17-19]. As the silicate ions (SiO_3^-) have been added to the media, they accumulate on the surface of the diatom and form $SiO_2(OH)_2^{2-}$ formula to become suitable for the diatom to absorb through a silica-receptor on their surface [24,25]. Therefore, the diatoms might release chemicals that can elevate the pH of the solution, as also experienced in our culturing progress in which the pH value increased from 7 to 8.5. The basis condition (high pH value) created a corrosion effect on the SiO_2 through the reaction (2).

$$SiO_2 + 2OH^- \rightarrow SiO_3^{2-} + H_2O \rightarrow SiO_2(OH)_2^{2-} \quad (2)$$

The presence of the silicic acid on the Si/SiO_2 spheres' surface led to the migration of the particles to the Si-receptor on the diatoms, making the diatom illuminated under the UV excitation. After 1 h cultivation, most *Chaetoceros sp.* cells were covered by Si/SiO_2 spheres (figure $4B_2$). By this process, aqueous silica was released from solid silica from Si/SiO_2 spheres and then diluted into the media indicating the diatom growth. After 2 h and 4 h, the concentration of the diatoms increased by their division; hence, it was possible to view less fluorescent diatoms under a microscope (figure $4C_2$,D_2).

Figure 5 shows the SEM of the Si/SiO_2 particles collected from the culturing media. It was observed that before interaction with *Chaetoceros sp.* cells in solution, the surface of the particles was smooth. After 1 h and 2 h in media, the surface of the particles became rough. Some crushed spikes visualized on the particles indicated that the particles were corroded (figure 5B,C). At 4 h growth of the diatom, blur effect could be seen on the SEM image of the Si/SiO_2 spheres that might correspond to an organic layer covering onto the particles, which may be the presence of the released chemical from the diatoms (figure 5D). The similar blur effect of SEM image on organic layer coated nanoparticles was observed by Tetsu's group [37]. The organic coat created an electron back-scattering effect, which made the SEM imaging become difficult. As consequence, blur effect might occur.

The delocalization of the SiO_2 particles on diatom-surface was also observed by Ikeda [23]. In this published article, the SiO_2 grains with the size in the range of 200 nm to 800 nm were

achieved by transmission electron microscopic (TEM) imaging, those attached on the surface of marine diatoms. The author also stated that this immobilization of the solid silica plays a very important role in biosilicification of the global silica cycle. The diatoms migrate to the larger solid silica sources such as soils or silica mine, and cause corrosion to increase aqueous silica level in natural water. After the biosilicification, silica in solid phase is accumulated in the diatom cell wall; hence with ocean currents; it would be dispersed into the ecosystem.

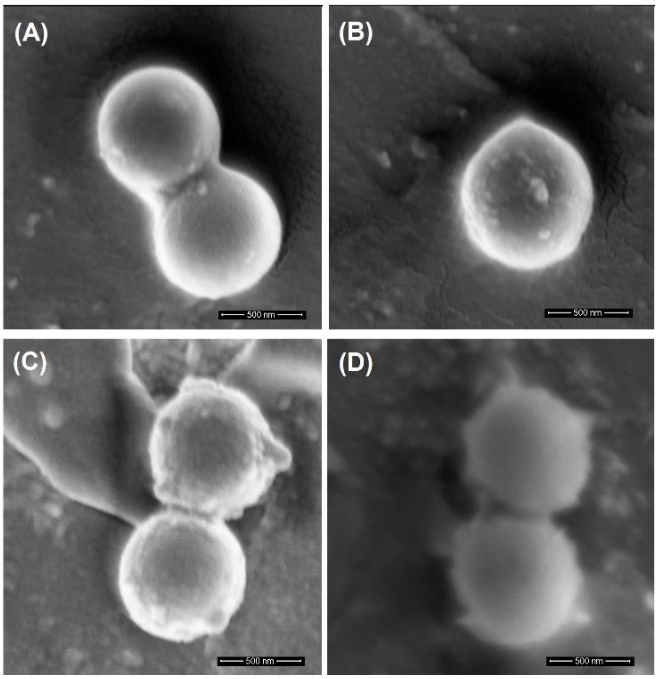

Fig. 5. SEM micrograph of the Si/SiO_2 spheres collected from the culturing media right after diatoms being added (A), after 1h (B), 2h (C) and 4h (D) cultivation.

Figure 6 introduces a simple method for monitoring the individual microalgae concentration during cultivation by light absorption. Typical absorption spectrum of a solution containing a $(6.52 \pm 1.58)\times10^6$ cells/mL *Chaetoceros sp.* – estimated from the counting chamber (Fig. 6A) – is measured in the 550-850 nm wavelength region as shown in Figure 6B. The peak at 685 nm corresponds to the characteristic absorption of Chlorophyll [38]. This peak has been applied as an indicator to measure the biomass level of the microalgae in aquaculture [39,40]. In this study, a calibration line was mapped showing the dependence of the *Chaetoceros sp.* concentration determined by cell counting chamber on the absorbance intensity observed at 685 nm (Fig. 6C). From the fitting parameters, the concentrations of the diatoms containing solution were estimated. Figure 6D shows the correlation between the estimated concentration value measured by spectrophotometer and by microscope in the range of 1×10^6 to 6×10^6 cells/mL. In the diagram, comparing to the line of equality, at the concentration value higher than 4.5×10^6 cells/mL, the estimated concentrations observed by the spectrophotometer were found greater than those by the cell counting chamber, which may be correspond to the multilayer of *Chaetoceros sp.* cells packed inside the counting chamber. Hence, in further diatom concentration measurement, if the absorbance at 685 nm more than 0.5, the diatoms containing solution has been diluted to 2 times before the concentration check by microscope.

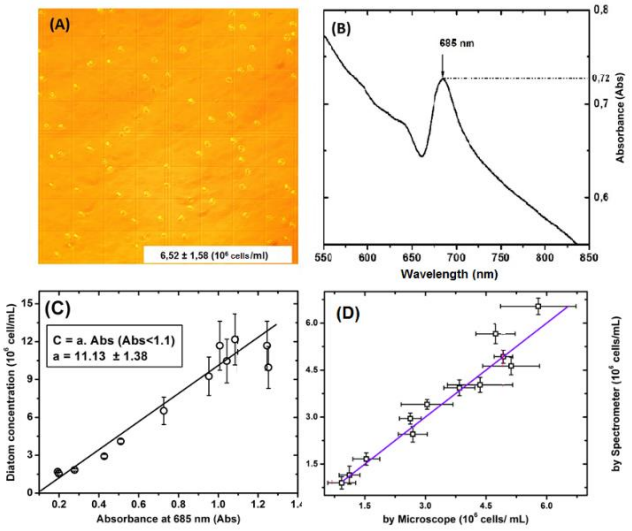

Fig. 6. Micrograph (A) and absorption spectrum at [550 nm – 850 nm] region of the *Chaetoceros sp.* containing sample at 6.52×10^6 cells/mL concentration. The dependence of diatom concentration on the absorbance at 685 nm (C) and the correlation between the concentrations measured by spectrophotometer and by microscope at the range from 1.2×10^6 to 6×10^6 cell/mL (D).

Figure 7 illustrates the change of the *Chaetoceros sp.* concentration during 4 days cultivation in different culturing media. The initial concentration of the diatoms in all the culturing process was 1.2×10^6 cells/mL. In conventional F2 media, the algae grew fast in the first 2 days, reached the maximum population after 3 days and started the death phase in the 4th day. This result agreed with the earlier result published by Tokushima [41]. By adding 15 mg, 30 mg and 120 mg of SiO_2 submicron-spheres, the molar concentration of the Si atom were about 2.5 times, 5 times and 20 times higher than that of in F2 media, respectively (see in Table 1); the diatoms grew faster. The growth rate in form of number divisions per day of the algae was calculated by the formula

$$d = \ln\frac{C_t}{C_0}\left(\frac{1}{t\ln 2}\right) \quad (3)$$

following the earlier studies [17,19,20], where the C_t, and C_0 are the concentration measured at times t and 0 respectively. Figure 7B demonstrates the dependence of as-calculated growth rates of the diatoms under in-this-study customized culturing media. The growth rates were experienced to decrease corresponding to the decrease of the relative media concentration in comparison with the concentration of the diatoms. From another perspective, the growth rate increased as the added amount of the SiO_2 particles increased, and reached 1.5 times higher than the growth rate calculated from the F2 media.

Some recent articles show that the growth rate of the diatom in solution did not increase as much during the elevation of the silica concentration [20,21,23]. In those studies, the added silica was in aqueous phase – in the form of silicate ion or of silicic acid. As we discussed above, at that high concentration those ions might create aggregation with the trace metals in

solution, and consequently cause the lack of nutrient to the media; hence, it might decrease the growth rate of the microalgae.

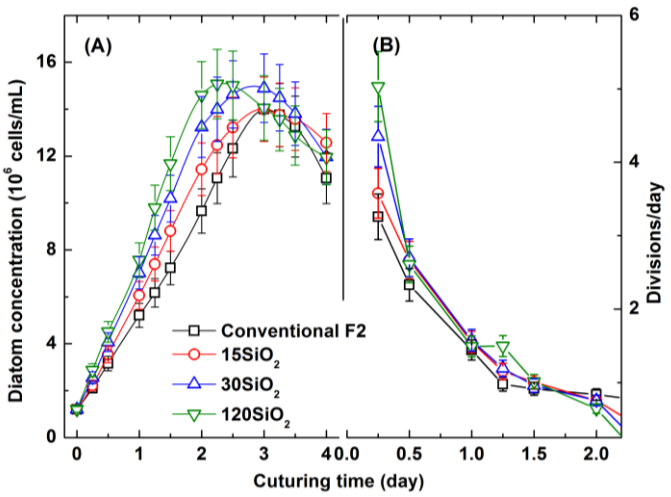

Fig. 7. The increase of the *Chaetoceros sp.* concentration during cultivation (A) and the change of division rate (B) in different solid-silica concentrations in comparison with conventional F2 culturing media.

Taking into account the silicic acid release from solid silica initiated by the diatoms, the high surface area of the SiO_2 nanoparticles not only increase the aqueous silica level in the culturing media, but also play as silica slow-release agent that indicates the high concentration of the silicic acid on the diatom surface. This is followed by the growth of the *Chaetoceros sp.* in solution. Therefore, the nanosize SiO_2 particles can be a good candidate for silica source for marine diatom cultivation, and might pave an appropriate way to develop the culturing media for higher growth rate diatom-accumulation.

4. Conclusion

To sum up, 720 nm mono-disperse Si/SiO_2 fluorescent submicron-spheres with narrow size-distribution were successfully synthesized in aqueous solution. Under the 356 nm light excitation, submicron particles emitted light-blue color with the spectrum centered at 440 nm, which could be monitored under a fluorescent microscope via the typical mode of the DAPI fluorophore for an investigation of extracellular biosilicification of *Chaetoceros sp.* The Si/SiO_2 particles migrated to the surface of the diatoms released silica in silicic acid form and being transported into the microalgae. This process created high concentration of aqueous silica at the diatoms' surface. As a consequence, the growth rate increased as the concentration of the SiO_2 particles was 120 mg/L, and reached 1.5 times higher than the growth rate calculated from the F2 media. The study not only presents a new-type of culturing media using SiO_2 nanoparticles for diatom cultivation, but also introduces a new aspect to the extracellular metabolism of microalgae biosilicification.

Acknowledgements

This study has been funded by the Vietnam National University, Hanoi under the project No. QG.19.08.

References

1. V. Smetacek., *Diatoms and the ocean carbon cycle*, Protist 150 (1999) 25-32.
2. B.P. Harvey, S. Agostini, K. Kon, S. Wada, J.M. Hall-Spencer, *Diatom dominate and alter marine food-webs when CO_2 rises*, Diversity 11(12) (2019) 242.
3. K. Leblanc, V. Cornet, P.R. Maury, O. Grosso, S.H. Nunige, C. Brunet et al., *Silicon cycle in the tropical South Pacific: contribution to the global Si cycle and evidence for an active pico-sized siliceous plankton*, Biogeosciences 15 (2018) 5595-5620.
4. V.A. Chepornov, C.G. Steiguber, P. Siegel, *Diatoms as hatchery feed: on-site cultivation and alternatives*, Hatcheryfeed 6(3) (2018) 23-27.
5. S.M. Rahman., G.A. Lutzu, Alam A., Sarker P., M.A.K. Chowdhury, A. Parsaimehr et al., *Microalgae in aquafeeds for a sustainable aquaculture industry*, J. Appl. Phycol. 30(1) (2018) 197-213.
6. Z. Yi, M. Xu, X. Di, S. Brynjolfsson, and W. Fu, *Exploring valuable lipids in diatoms*, Front. Mar. Sci. 4 (2017) 17. doi: 10.3389/fmars.2017.00017.
7. K. Seth, A. Kumar, R.P. Rastogi, M.Meena., V. Vinayak., Harish, *Bioprospecting of flucoxanthin form diatoms – Challenges and perspectives*, Algal Res. 60 (2021) 102475.
8. M.J. Khan, A. Rai, A. Ahirwar, V. Sirotiya, M. Mourya, S. Mishra et al., *Diatom microalgae as smart nanocontainers for biosensing wastewater pollutants: recent trends and innovations*, Bioengineered 12(2) (2021) 9531-9549.
9. M. Terracciano., L.D. Stefano, I. Rea., *Diatom green nanotechnology for biosilica-based drug delivery systems*, Pharmaceutics 10(4) (2018) 242.
10. B. Delalat, V.C. Sheppard, S.R. Ghaemi, S. Rao, C.A. Prestidge, G. Mcphee et. al., *Targeted drug delivery using genetically engineered diatom biosilica*, Nat. Commun. 6 (2015) 8791.
11. A. Kamińska, M. Sprynskyy, K. Winkler, T. Szymborski, *Ultrasensitive SERS immunoassay based on diatom biosilica for detection of interleukins in blood plasma*, Anal. Bioanal. Chem. 409 (2017) 6337-6347.
12. X. Kong, X. Chong, K. Squire., A.X. Wang, *Microfluidic diatomite analytical devices for illicit drug sensing with ppb-level sensitivity*, Sensors and Actuators B 259 (2018) 587-595.
13. K.K. Sharma, H. Schuhmann, P.M. Schenk, *High lipid induction in microalgae for biodiesel production*, Energy 5 (2012) 1532-1553.
14. U. Karsten, R. Schumann, S. Rothe, I. Jung, L. Medlin, *Temperature and light requirement for growth of two diatom species (Bacillariophyceae) isolated from an Acrtic macroalga*, Polar Biol. 29 (2006) 476-486.
15. T. Lebeau, J.M. Robert, *Diatom cultivation and biotechnologically relevant products. Part I: Cultivation at various scales*, Appl. Microbiol. Biotech. 60 (2003) 612-623.
16. L. Provasoli, A.D. Agostino, *Development of artificial media for Artemia salina*, Bio. Bull. 136 (1969) 434-453.
17. R.R.L. Guilard, J.H. Ryther, *Studies of marine planktonic diatoms: I. Cyclotella nana hustedt, and Detonula confervacea (Cleve) gran*, Can. J. MicroBiol., 8 (1962) 229-239.
18. D.C. Ohnemus, J.W. Krause, M.A. Brzezinski, J.L. Collier, S.B. Baines, B.S. Twining, *The chemical form of silicon in marine Synechococcus*, Mar. Chem. 206 (2018) 44-51.
19. R. Tostevin, J.T. Snow, Q. Zhang, N.J. Tosca, R.E.M. Rickaby, *The influence of elevated SiO_2 (aq) on intracellular silica uptake and microbial metabolism*, Geobiology 19(4) (2021) 421-433.
20. M.A. Brezezinski, J.W. Krause, S.B. Baines, J.L. Collier, D.C. Ohnemus, B.S. Twinning, *Patterns and regulation of silicon accumulation in Synechococcus Spp.*, J. Phycol. 53(4) (2017) 746-761.
21. S.B. Baines, B.S. Twinning, M.A. Brezezinski, J.W. Krause, S. Vogt, D. Assael et al., *Significant silicon accumulation by marines*

picocyanobacteria, Nat. Geosci. 5 (2012) 886-891.

22. G.D. Okcu, E. Eustance, Y.S. Lai, B.E. Rittmann, *Evaluation of co-culturing a diatom and a coccothophor using different silicate concentrations*, Sci. Total Environ. 15 (2021) 145217.
23. T. Ikeda, *Bacterial biosilicification: a new insight into the global silicon cycle*, Biosci. Biotechnol. Biochem. 25 (2021) 1324-1331.
24. M. Hilderbrand, *Silicic acid transport and its control during cell wall silicification in diatom*, Weley-VCH German: Verlag GmbH & Co. KGaA, 2004.
25. H.S. Oh, S.E. Lee, C.S. Han, J. Kim, O. Nam, S. Seo et al., *Silicon transporter genes of Fraggilariposis cylindrus (Bacillariophyceae) are differentially expressed during the progression of cell cycle synchronized by Si or light*, Algae 33 (2018) 191-203.
26. Y. Ma, Y. Li, X. Zhong, *Silica coating of luminescent quantum dots prepared in aqueous media for cellular labeling*, Mat. Res. Bulletin 60 (2014) 543-551.
27. S.T. Selvan, *Silica-coated quantum dots and magnetic nanoparticles for bioimaging applications (Mini-Review)*, Biointerphases 5(3) (2010) FA110-5.
28. S. Saita, H. Kawasaki, *Origin of the fluorescence in silica-based nanoparticles synthesized from aminosilane coupling agent*, J. Luminescence 232 (2021) 117849.
29. Y. Zhong, F. Peng, F. Bao, S. Wang, X. Ji, Y. Su et al., *Large-scale aqueous synthesis of fluorescent and biocompatible silicon nanoparticles and their use as highly photostable biological probes*, J. Am. Chem. Soc. 135 (2013) 8350-8356.
30. J.H. Lim, S.W. Ha, J.K. Lee, *Precise size control of silica nanoparticles via alkoxy exchange equilibrium of tetraethyl orthosilicate (TEOS) in the mixed alcohol solution*, Bull. Korean Chem. Soc., 33 (2012) 1067-1070.
31. A.S. Afifah, I.W.K. Suryawan, A. Sarwono, *Microalgae production using photo-bioreactor with intermittent aeration for municipal wastewater substrate and nutrient removal*, Commun. Sci. Technol., 5(2) (2020) 107-111.
32. B.V. Oliinyk, D. Korytko, V. Lysenko, S. Alekseev, *Are fluorescent silicon nanoparticles formed in a one-pot aqueous synthesis?*, Chem. Mat. 31 (2019) 7167-7172.
33. K. Talreja, I. Chauhan, A. Ghosh, A. Majumdar, B.S. Butola, *Functionalization of silica particles to tune the impact resistance of shear thickening fluid treated aramid fabric*, RSC Adv. 7 (2017) 48787-49794.
34. V. Divya, B. Agrawal, A. Srivastav, P. Bhatt, S. Bhowmik, Y.K. Agrawal et al., *Fluorescent amphiphilic silica nanopowder for developing latent fingerprints*, Aus. J. Foren. Sci. 3 (2018) 354-367.
35. C. Wurth, M. Grabolle, J. Pauli, M. Spieles, *Relative and absolute determination of fluorescence quantum yield of transparent samples*, Nat. Protoc. 8 (2013) 1535-1550.
36. L.M.T. Phan, S. H. Baek, T.P. Nguyen, K.Y. Park, S. Ha, R. Rafique et al., *Synthesis of fluorescent silicon quantum dots for ultra – rapid and seclective sensing of Cr(VI) ion and biomonitoring of cancer cells*, Mater. Sci. Eng. C 93 (2018) 429-436.
37. T. Yonezawa, H. Tsukamoto, M. Matsubara, *Low-temerature nanoredox two-step sintering of gelatin nanoskin-stabilized submicrometer-sized copper fine particles for preparing highly conductive layer*, RSC. Adv. 5 (2015) 61290-61297.
38. P. Kuczynska, M.J. Rzeminska, K. Strzalka, *Photosynthetic pigment in diatoms*, Mar. Drug. 13 (2015) 5847-5881.
39. D.U.S. Ballardo, S. Rossi, V. Hernandez, R.V. Gomes, M.C.R. Unceta, J.C. Corrales et al., *A simple spectrophotometric method for biomass measurement of important microalgae species in aquaculture*, Aquac. 448 (2015) 87-92.
40. G.N. Hotos, D. Avramidu, V. Bekiari, *Calibration curves of culture density assessed by spectrophotometer for three microalgae (Nephosemis sp., Amphidinium carterae and Phormidium sp.)*, European J. Biol. Biotech. 1(6) (2020) 1-7.
41. H. Tokushima, N.I. Kashino, Y. Nakazato, A. Masuda, K. Ifuku, Y. Kashino, *Advantagous characteristics of the diatom Chaetoceros gracillis as a sustainable biofuel producer*, Biotechnol. Biofuel. 9 (2016) 235.